ON THE PROPAGATION VELOCITY OF SWIRL WAVES IN ANNULAR FLOWS

Alp Albayrak, Wolfgang Polifke

Professur für Thermofluiddynamik, Technische Universität München,
Boltzmannstr. 15, D-85748 Garching, Germany
email: albayrak@tfd.mw.tum.de

The impact of swirl fluctuations on flame dynamics has been investigated by several authors and results suggest that the overall flame response is governed by superposition of two or more flow-flame-acoustic interaction mechanisms. In this context, the relative phases of the individual contributions must be described accurately, which in turn implies that the propagation velocities of the various perturbations must be known. While acoustic waves propagate with the speed of sound, it is generally assumed that fluctuations of swirl are convected by the bulk flow and thus propagate with the mean flow velocity. However, in both experiments and numerical simulations it was observed repeatedly that the propagation speed of swirl waves may be noticeably higher than the bulk flow velocity. In the present work a formulation for the propagation speed is proposed, which is based on inviscid theory of confined swirling flows. The resulting formula consists of two propagation modes with faster and slower speeds than the flow velocity. Moreover, it is established that the azimuthal velocity and the duct size have significant impact on the propagation speed of swirl fluctuations. In contrast to the constant propagation speed assumption, the new model depends on the radial position. The importance of the radial momentum balance for the propagation is emphasized. A validation study is performed by comparing the results against 2-D Large Eddy Simulations. For this purpose the step responses to azimuthal velocity perturbations are examined. The resulting time-lag model can be introduced to low order models for the estimation of combustion instabilities.

1. Introduction

The use of swirl in combustion systems is the key point for stabilizing the flame by reheating the cold premixture through the re-circulation zones formed by vortex breakdown phenomenon. At the same time, the swirling flow completely changes both flow and flame structures and their interaction [1, 2]. Therefore it is essential to understand the physics behind the swirling flow in combustion in order to predict the instability in the system.

One parameter that has an important impact on the flame response is the swirler position [2, 3]. By changing the swirler position, the flame dynamics can be altered by the interference between the axial and tangential velocity perturbations, which have by nature completely different time scales. This phenomenon has been studied by means of experiments and numerical simulations by Komarek *et al.* [3].

The axial velocity perturbations u'_x associated with the acoustic waves in the system travel in longitudinal direction "x" with wave speed $\bar{u}_x \pm c$, where $\bar{u}_x$ is the mean axial flow velocity and c is the speed of sound. For the tangential velocity perturbations u'_θ, it is assumed that they propagate in the longitudinal direction with the mean axial flow velocity $u_p = \bar{u}_x$. Since the mean axial flow velocities in combustion systems are at least one order of magnitude smaller than the speed of sound, there is a huge difference between the time scales corresponding to the propagation of axial and tangential velocity perturbations.

Several authors [3–6] assumed that tangential velocity perturbations propagate with the convective flow velocity. Since their approach was limited to 1-D, the convective velocity is assumed to be equal to the constant bulk velocity, which neglects the radial distribution of axial velocity. The propagation speed assumption as constant bulk velocity is not matching with experiments and simulation results. For example, Komarek *et al.* [3] measured the mean flow velocity after the swirler as $\bar{u}_x = 11.3$ m/s, but the tangential velocity perturbations caused by the swirler propagate with a speed $u_p = 19.5$ m/s. This discrepancy stimulated the authors of the present paper to build a better model in order to estimate the propagation speed more accurately.

A new formula based on the inviscid theory of confined swirling flows is adopted to estimate u_p. The fundamental theory is proposed by Greitzer *et al.* [7, 8] to estimate the expansion of vortex cores in unconfined and confined cylindrical ducts. With slight modifications, a new formula for u_p is proposed and validated against 2-D LES simulations.

2. Theory

Greitzer studied the vortex core expansion in cylindrical flows by using the inviscid theory of confined swirling flows. In his work the tangential velocity profile is modeled as a Rankine vortex, whose core is characterized as a forced vortex and the outer region as a free vortex. The filament that separates the forced vortex from the free vortex defines two control volumes for core and outer regions. By solving linearized equations for mass and momentum combined with a simplified radial momentum balance, the fluctuations in filament location can be estimated, which are then related with the expansion behavior of the core flow.

A similar approach is used to estimate the propagation speed of azimuthal velocity perturbations. In the present work it is not physical to assume a Rankine vortex for annular swirling flow after a swirler. Therefore, there exists no distinct transition between the forced and free vortex, where the filament is supposed to be placed. In the current approach, filaments stemming from each radius are tracked instead of tracking only one of them. Therefore, the filament position "a" is regarded as a variable in the analysis. Varying filament position results in different control volumes, for which linearized conservation equations are solved. By finding dispersion relation for linearized conservation equations as described by Greitzer, the propagation speed is estimated as a phase velocity. It is assumed that fluctuations in filament position are caused by tangential velocity perturbations, therefore the estimated speed is also related to the propagation of azimuthal velocity perturbations.

The approach is applied to swirling flow in an annular cylindrical duct located after a swirler, which is modeled as 2-D axisymmetric flow (shown in fig. 1) with the following assumptions;
  – Incompressibility $\rho = const.$,
  – Inviscid flow $\nu = 0$,
  – 2-D axisymmetric swirling flow. The azimuthal derivatives vanish $\frac{\partial (.)}{\partial \theta}$,
  – Radial flow velocity is small. $u_r = 0$.
Inflow velocities are modeled as uniform profiles both in axial $u_x(r) = u_x$ and azimuthal direction $u_\theta(r) = u_\theta$. But, it is also possible to carry out the same analysis with different velocity profiles, i.e free vortex, Rankine vortex and others, which result in different propagation speeds due to the different radial pressure profiles obtained by eq. (1).
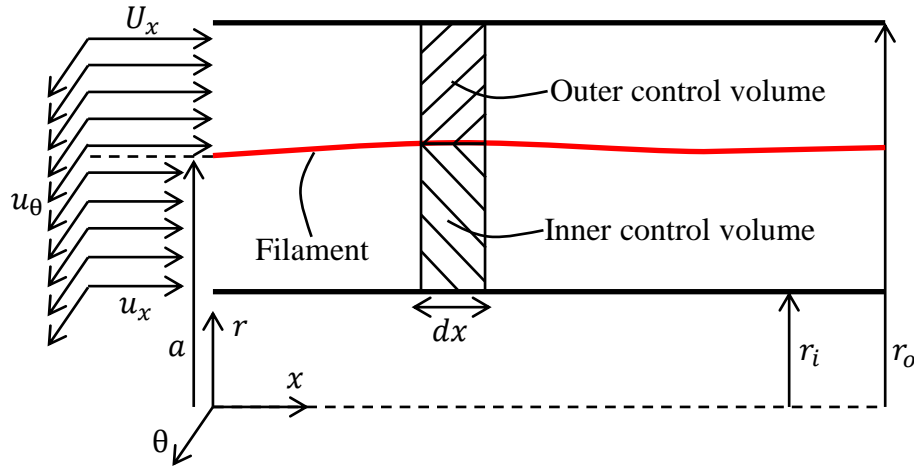
Figure 1: 2-D configuration of axisymmetric swirling flow

Under the given assumptions, the radial momentum conservation equation is simplified to

$$\frac{\partial p}{\partial r} = \rho \frac{u_\theta^2}{r},$$

(1)

which can be easily integrated as

$$p(r) - p_{r_i} = \rho u_\theta^2 \ln \frac{r}{r_i},$$

(2)

where p_{r_i} is the pressure at the inner wall. It is also possible to use the pressure at the outer wall p_{r_o} instead of the inner wall for the integration.

The conservation of mass and momentum equations for the inner control volume ($r < a$) read, respectively

$$\frac{\partial (A)}{\partial t} + \frac{\partial (Au_x)}{\partial x} = 0,$$

(3)

$$\frac{\partial (Au_x)}{\partial t} + \frac{\partial (Au_x^2)}{\partial x} = -\frac{A}{\rho} \frac{\partial (p_a)}{\partial x},$$

(4)

where $A = \pi (a^2 - r_i^2)$ is the area of the inner control volume, u_x is the axial velocity in the inner region and p_a is the pressure at the selected filament.

Similarly, the conservation of mass and momentum equations for the outer control volume ($r > a$) read, respectively,

$$\frac{\partial (A_D - A)}{\partial t} + \frac{\partial [(A_D - A) U_x]}{\partial x} = 0,$$

(5)

$$\frac{\partial (A_D - A) U_x}{\partial t} + \frac{\partial [(A_D - A) U_x^2]}{\partial x} = -\left(\frac{A_D - A}{\rho}\right) \frac{\partial (p_a)}{\partial x} + \left[\frac{(A_D - A) u_\theta^2}{2 (A + \pi r_i^2)}\right] \frac{\partial A}{\partial x},$$

(6)

where $A_D = \pi (r_o^2 - r_i^2)$ is the total area of the duct and U_x is the axial velocity of the outer region.

In order to examine the small amplitude perturbations analytically, the eqs. (3)–(6) are linearized by expanding all variables $q = \bar{q} + q'$ by their mean $\bar{q}$ and fluctuating parts q'. The linearized equations read as

$$\frac{\partial (A')}{\partial t} + \bar{u}_x \frac{\partial (A')}{\partial x} + \bar{A} \frac{\partial (u_x')}{\partial x} = 0,$$

(7)

(8)
$$\frac{\partial \left(u'_x\right)}{\partial t} + \bar{u}_x \frac{\partial \left(u'_x\right)}{\partial x} + \frac{1}{\rho} \frac{\partial \left(p'_a\right)}{\partial x} = 0,$$

(9)
$$\frac{\partial \left(A'\right)}{\partial t} + \bar{U}_x \frac{\partial \left(A'\right)}{\partial x} - \left(A_D - \bar{A}\right) \frac{\partial \left(U'_x\right)}{\partial x} = 0,$$

(10)
$$\frac{\partial \left(U'_x\right)}{\partial t} + \bar{U}_x \frac{\partial \left(U'_x\right)}{\partial x} + \frac{1}{\rho} \frac{\partial \left(p'_a\right)}{\partial x} - \frac{u_\theta^2}{2 \left(\bar{A} + \pi r_i^2\right)} \frac{\partial \left(A'\right)}{\partial x} = 0.$$

Linearization results in four partial differential equations for the variables (A', u'_x, U'_x, p'_a), therefore the system of partial differential equations is complete. The eigenmodes of the equations can be calculated by applying the ansatz

(11)
$$\begin{bmatrix} A' \\ u'_x \\ U'_x \\ p'_a \end{bmatrix} = \begin{bmatrix} A_0 \\ u_{x_0} \\ U_{x_0} \\ p_{a_0} \end{bmatrix} e^{i(kx - \omega t)},$$

where $A_0, u_{x_0}, U_{x_0}, p_{a_0}$ are the constant amplitudes for corresponding variables, k is the wave number in the axial direction and ω is the angular frequency.

Substituting eq. (11) in the linearized conservation eqs. (7)–(10) leads to four algebraic equations, whose determinant must be equal to zero for non-trivial solution. This eigenvalue problem results in a dispersion relation, which can be solved for the phase velocity ω/k as

(12)
$$\frac{\omega}{k} = \frac{\left(A_D - \bar{A}\right) \bar{u}_x + A \bar{U}_x}{A_D} \pm \sqrt{\left(1 - \frac{\bar{A}}{A_D}\right) \left[\frac{u_\theta^2 \bar{A}}{2 \left(A + \pi r_i^2\right)} - \frac{\bar{A}}{A_D} \left(\bar{U}_x - \bar{u}_x\right)^2\right]},$$

where the angular frequency is a real valued linear function of the wave number. This is an exceptional case for the stability analysis. Perturbations are neither growing nor decaying and the propagation speed is the only information that can be obtained from the analysis. The equation can be further simplified by setting the axial velocities of inner and outer part to be equal $\bar{U}_x = \bar{u}_x$ and substituting $A = \pi \left(a^2 - r_i^2\right)$ and $A_D = \pi \left(r_o^2 - r_i^2\right)$. The resulting formula reads as

(13)
$$u_p \left(a\right) = \bar{u}_x \pm u_\theta \sqrt{\frac{\left(r_o^2 - a^2\right) \left(a^2 - r_i^2\right)}{2a^2 \left(r_o^2 - r_i^2\right)}},$$

where $u_p = \omega/k$ is called as the propagation speed for the perturbed quantities in eq. (11).

3. Interpretation

Although the azimuthal velocity u_θ does not show up in eq. (11) as a perturbed quantity, it is reasonable to surmise that fluctuations in the filament location are related to the azimuthal velocity perturbations. The radial pressure gradient depends strongly on azimuthal velocity, as seen in eq. (1). Perturbations in azimuthal velocity change the radial pressure gradient, which causes the filament to be relocated. Therefore, the propagation speed u_p is relevant for azimuthal velocity perturbations.

The propagation speed here consists of two modes with faster and slower propagation speeds. The radial momentum conservation equation eq. (1) is responsible for the presence of these modes. The impact of the radial pressure gradient can be seen in the last term on the right hand side of the eq. (10). In the absence of azimuthal velocity, the radial momentum equation has only the trivial solution, i.e.

the radial pressure gradient being zero. In this case the perturbation is only convected with the axial flow velocity.

The amount by which the propagation speed differs from the convective speed is specified by the second term on the right hand side of eq. (13), which depends on the azimuthal velocity u_θ, the duct geometry r_i, r_o and the radius a. Different control volumes formed by radial variations of the filament location result in different propagation velocities. Therefore, it is plausible to plot the two propagation speeds as functions of radius (see fig. 2). It is shown that both fastest and the slowest propagation speeds occur at same filament location, namely at $a = \sqrt{r_i r_o}$ and the corresponding propagation speeds are

$$(14) \qquad u_p \left(\sqrt{r_i r_o} \right) = u_x \pm u_\theta \sqrt{\frac{(r_o - r_i)}{2 (r_o + r_i)}}.$$

The fastest and slowest propagation speeds are important for the validation cases in section 4, because it is easy to deduce from experiments and numerical simulations, when the perturbation starts acting and vanishes.
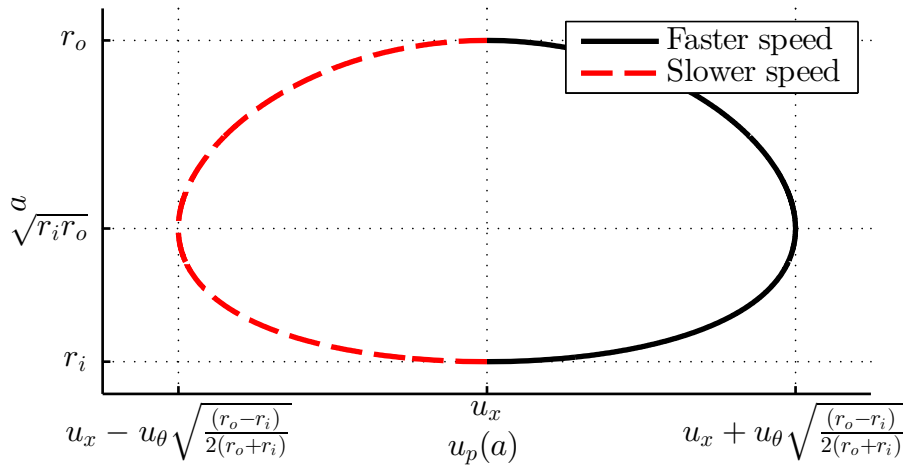

Figure 2: Propagation speed versus filament position

4. Validation

The validation of the model is achieved by comparing step responses estimated by the model and 2-D CFD simulations of an annular duct. The step response is the response of the system to the input as Heaviside function.

The response $h(t)$ is defined as

$$(15) \qquad \frac{\int_{r_i}^{r_o} 2\pi r u_\theta' (\Delta x, r, t) \, dr}{\int_{r_i}^{r_o} 2\pi r \bar{u}_\theta (\Delta x, r) \, dr} = \frac{\int_0^\infty h(\tau) \left(\int_{r_i}^{r_o} 2\pi r u_\theta' (0, r, t - \tau) \, dr \right) d\tau}{\int_{r_i}^{r_o} 2\pi r \bar{u}_\theta (0, r) \, dr},$$

where the term in brackets on right hand side is the system input as the area averaged azimuthal velocity perturbation imposed at inflow ($x = 0$) and the left hand side term is the system output as area averaged azimuthal velocity fluctuations after Δx distance. Both terms are nondimensionalized with terms in denominators. The response is called as step response if the perturbation at the inflow is imposed as a Heaviside function $u_\theta' (0, r, t) = \varepsilon \bar{u}_\theta(0) H(t)$, where ε is a small real value.

For the analytical models the step response can be further simplified as

$$(16) \qquad h(t) = \frac{1}{A_D} \int_{r_i}^{r_o} 2\pi r H \left(t - \frac{\Delta x}{u_p(r)} \right) dr.$$

The constant propagation assumption $u_p = \bar{u}_x$ yields to $h(t) = H(t - \Delta x/\bar{u}_x)$, which is shifted Heaviside function and shown in fig. 3.

2-D incompressible LES simulations are performed with the CFD software OpenFOAM. The inflow velocity boundary conditions are assumed to be uniform as schematically described in fig. 1. Slip wall boundary condition is applied on duct walls. The azimuthal velocity at the inflow is perturbed by broad-band signal. The step response of the system is estimated (for details refer [9, 10]). In the step response, the time lag corresponding to the first non-zero value is associated with the fastest propagation speed and the time lag corresponding to the settling to the new steady value is associated with the slowest propagation speed. The propagation speed can be computed by dividing the distance between input and output planes by the time lag from the step response.

4.1 Validation against 2-D axisymmetric Navier-Stokes numerical simulations

The geometry and the bulk flow velocity of the reference test case correspond to the BRS burner duct that was numerically and experimentally analyzed by Komarek *et al.* [3]. The inner and outer radii are respectively, $r_i = 8$ mm and $r_o = 20$ mm, the axial and azimuthal velocities are assumed to be uniform and equal $u_x = U_x = u_\theta = 11.3$ m/s. Broadband perturbations in azimuthal velocity are imposed at the inflow and the area averaged azimuthal velocity is measured 50 mm after inflow. The estimated step response is shown in fig. 3a. The time is nondimensionalized by diving it to the reference time $t_{ref} = u_x/\Delta x$. The reference time is the propagation time lag that is computed with the constant propagation speed assumption between the input and output planes.

The propagation speed u_p depends on the azimuthal velocity u_θ and inner and outer radii of the duct. In order to validate these dependencies, two more cases are considered. In one case the azimuthal velocity is halved $u_\theta = 5.65$ m/s and in the other one the inner radius of the duct is doubled $r_i = 16$ mm. The corresponding step responses are plotted in fig. 3b for the case with halved azimuthal velocity and in fig. 3c for the case with doubled inner radius.

The step response results show that the constant propagation speed assumption is inadequate and not able to capture the nature of the propagation process. Good agreement is achieved with the new model in all three cases (see figs. 3a–3c), especially for the fastest and the slowest propagation speeds.

By comparing fig. 3a with fig. 3b, the dependency of the propagation speed on the inner radius is examined. Increasing the inner radius decreases the additional term of the propagation speed, which resuts in narrower response. Similarly, decreasing azimuthal velocity results in narrower response (see figs. 3a and 3c).

Although the shapes of step responses are not matching perfectly, the proposed model gives a new level of understanding for the propagation mechanism. It is found out that the propagation consist of two modes with different speeds and they depend not only on the radial position but also on the azimuthal velocity and the size of the duct.

5. Conclusion

A new formula describing the propagation of azimuthal velocity perturbations is derived from the inviscid theory of swirling flows presented by Greitzer [8]. The propagation speed is determined by analyzing fluctuations in the filament position, i.e solving the linearized mass and momentum conservation equations combined with the simplified radial momentum equation on the control volumes that are separated by filaments. The fluctuations in the filament location are related with the propagation of the azimuthal velocity perturbations via radial pressure gradient. It is shown that the azimuthal velocity perturbations propagate as wave motion, which contains faster and slower speeds compared to the axial flow velocity.

The constant propagation speed assumption is shown to be unsatisfactory, especially for the cases with different azimuthal velocity and size. This explains why several authors [3–6] encounter different propagation speeds for different geometries and swirlers. With the present model it is possible
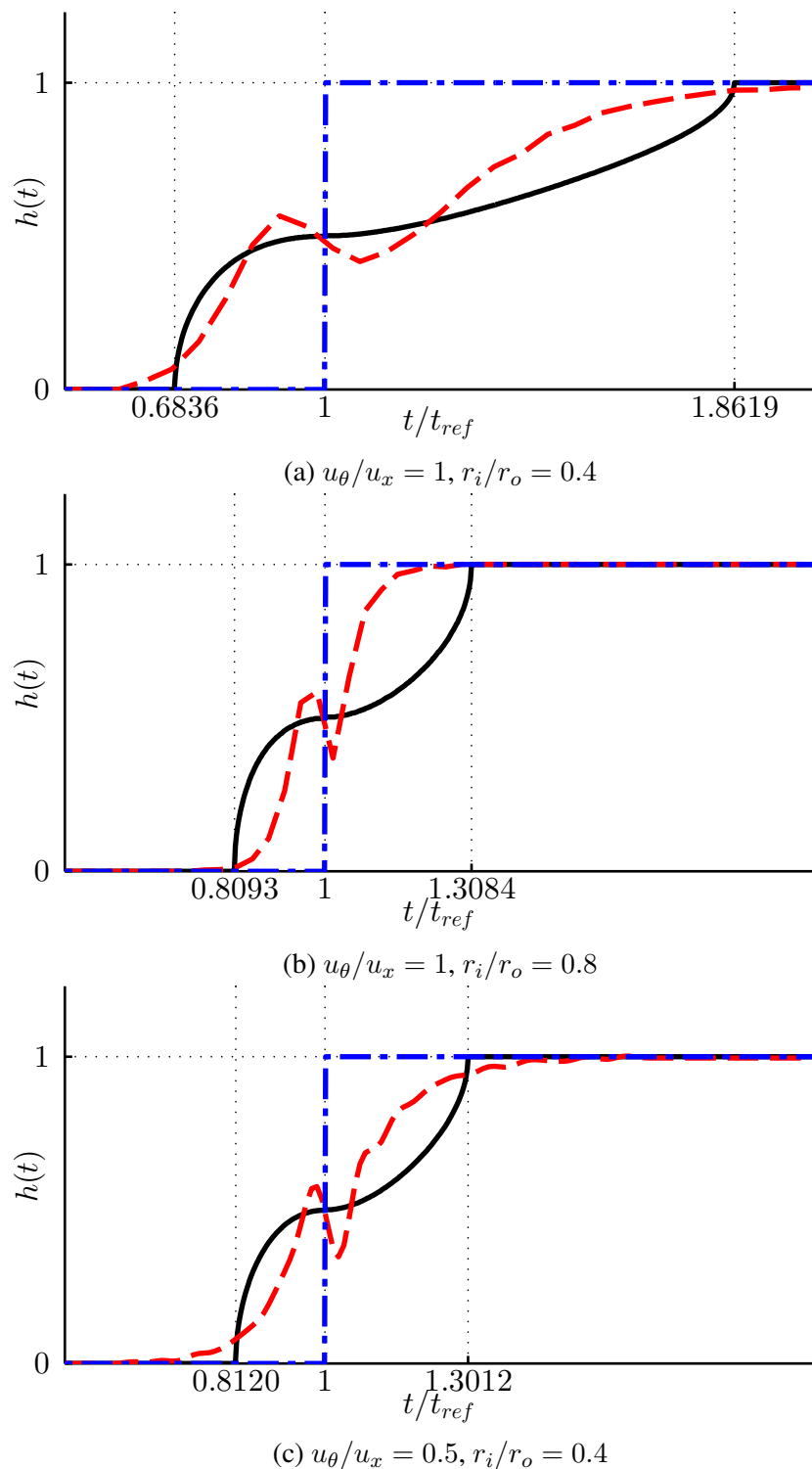
(a) $u_\theta/u_x = 1$, $r_i/r_o = 0.4$

(b) $u_\theta/u_x = 1$, $r_i/r_o = 0.8$

(c) $u_\theta/u_x = 0.5$, $r_i/r_o = 0.4$

Figure 3: Step responses of the azimuthal velocity perturbation for constant propagation speed model (——·——), present model (———) and CFD result (—— ——·). $u_x = 11.3$ m/s, $r_o = 20$mm.

to calculate the propagation speed more precisely for different geometries and different azimuthal velocities. This is shown in fig. 3, where a parameter study is performed by changing the azimuthal velocity and inner radius of the duct.

The present investigation is important for the prediction of the combustion instabilities. The difference in time scales for different physical phenomena is one of the key factors that control flame dynamics, in particular strength of flame response. The time scale related with the axial velocity perturbation that propagates with the speed of sound are at least one order of magnitude less than the

time scale related with the azimuthal velocity perturbation that propagates with flow velocity. The present model enables a better understanding of propagation of azimuthal velocity perturbations that might be useful to predict the combustion instabilities more accurately. One key point of this analysis is the response to the azimuthal velocity perturbations is weaker but longer in time compared to the response with constant speed assumption. This is due to the spreading of the perturbation caused by different propagation speeds.

Acknowledgements

References

1. N. Syred and J. Beér, "Combustion in Swirling Flows: A Review," *Combustion and Flame*, vol. 23, no. 2, pp. 143–201, 1974.

2. D. Straub, G. Richards, M. Yip, W. Rogers, and E. Robey, "Importance of axial swirl vane location on combustion dynamics for lean premix fuel injectors," in *Joint Propulsion Conferences*, American Institute of Aeronautics and Astronautics, 1998.

3. T. Komarek and W. Polifke, "Impact of Swirl Fluctuations on the Flame Response of a Perfectly Premixed Swirl Burner," *Journal of Engineering for Gas Turbines and Power*, vol. 132, no. 6, 2010.

4. P. Palies, D. Durox, T. Schuller, and S. Candel, "Experimental Study on the Effect of Swirler Geometry and Swirl Number on Flame Describing Functions," *Combustion Science and Technology*, vol. 183, no. 7, pp. 704–717, 2011.

5. P. Palies, D. Durox, T. Schuller, and S. Candel, "Acoustic-convective mode conversion in an aerofoil cascade," *Journal of Fluid Mechanics*, vol. 672, pp. 545–569, 2011.

6. V. S. Acharya and T. C. Lieuwen, "Role of Azimuthal Flow Fluctuations on Flow Dynamics and Global Flame Response of Axisymmetric Swirling Flames," in *AIAA SciTech*, American Institute of Aeronautics and Astronautics, 2014.

7. D. L. Darmofal, R. Khan, E. M. Greitzer, and C. S. Tan, "Vortex core behaviour in confined and unconfined geometries: a quasi-one-dimensional model," *Journal of Fluid Mechanics*, vol. 449, pp. 61–84, 2001.

8. E. M. Greitzer, C. S. Tan, and M. B. Graf, *Internal Flow: Concepts and Applications*, vol. 3. Cambridge University Press, 2004.

9. W. Polifke, A. Poncet, C. Paschereit, and K. Döbbeling, "Reconstruction of acoustic transfer matrices by instationary computational fluid dynamics," *Journal of Sound and Vibration*, vol. 245, no. 3, pp. 483–510, 2001.

10. W. Polifke and A. Gentemann, "Order and realizability of impulse response filters for accurate identification of acoustic multi-ports from transient CFD," *Int. J. of Acoustics and Vibration*, vol. 9, no. 3, pp. 139–148, 2004.